

## RESEARCH ARTICLE

 OPEN ACCESS

Received: 30.09.2021

Accepted: 12.12.2021

Published: 22.12.2021

**Citation:** Prasad M, Kempaiah UN, Mohan RM, Nagaral M (2021) Microstructure, Tensile and Compression Behaviour of AlSi10Mg Alloy Developed by Direct Metal Laser Sintering. Indian Journal of Science and Technology 14(45): 3346-3353. <https://doi.org/10.17485/IJST/v14i45.1705>

\* **Corresponding author.**[mailrmp@gmail.com](mailto:mailrmp@gmail.com)**Funding:** None**Competing Interests:** None

**Copyright:** © 2021 Prasad et al. This is an open access article distributed under the terms of the [Creative Commons Attribution License](https://creativecommons.org/licenses/by/4.0/), which permits unrestricted use, distribution, and reproduction in any medium, provided the original author and source are credited.

Published By Indian Society for Education and Environment ([iSee](https://www.isee.org/))

**ISSN**

Print: 0974-6846

Electronic: 0974-5645

# Microstructure, Tensile and Compression Behaviour of AlSi10Mg Alloy Developed by Direct Metal Laser Sintering

Manjunath Prasad<sup>1\*</sup>, U N Kempaiah<sup>2</sup>, R Murali Mohan<sup>3</sup>, Madeva Nagaral<sup>4</sup><sup>1</sup> Research Scholar, Department of Mechanical Engineering, UVCE, Bangalore 560001<sup>2</sup> Professor, Department of Mechanical Engineering, UVCE, Bangalore 560001<sup>3</sup> Assistant Professor, Department of Mechanical Engineering, Deputy Manager, Government Engineering College, Hassan, 573202<sup>4</sup> Deputy Manager, Aircraft Research and Design Centre, HAL, Bangalore 560037

## Abstract

**Objective:** To evaluate the tensile and compression behaviour of Al-Si10-Mg alloy developed by selective laser melting (SLM) process. **Method:** Al-Mg10-Si alloy developed by SLM process along XY (45°) and Z (90°) orientations. These prepared samples were subjected to microstructural characterization by SEM and EDS. Mechanical properties like tensile and compression behaviours were evaluated according to ASTM standards. **Findings:** Microstructural studies revealed the effect of grains on the mechanical behaviour of Al-Mg10-Si alloy built in XY (45°) and Z (90°) orientations. EDS analysis confirmed the presence of Mg and Si elements in the Al matrix. Tensile strength of Al-Mg10-Si alloy built in XY (45°) orientation is 428.6 MPa against 408.3 MPa in Z (90°) orientations developed samples. Further, compression strength of samples developed in XY (45°) orientation is more than that of developed in Z (90°) orientations. **Novelty:** In the current study Al-Mg10-Si alloy samples were produced by selective laser melting method in XY (45°) and Z (90°) orientations. Very minimal investigations were carried out on Al-Mg10-Si alloy specimens built in XY (45°) orientation.

**Keywords:** AlMg10Si Alloy; Microstructure; Tensile Behaviour; Compression Strength; Build Orientation

## 1 Introduction

Additive manufacturing is as of now applied across an expansive material determination and it is filling production volume and monetary effect<sup>(1-3)</sup>. Aluminum is one of the materials that assume a huge part in the avionic business due to its great solidarity to-weight proportion<sup>(4-6)</sup>. The advancement of metal AM methods has gained extraordinary headway from that point forward, yet faces novel handling and materials improvement issues. Understanding the different cycles used to make metal AM parts, and the issues related with them, is basic to working on the abilities of the equipment and the materials that are delivered. A few specialists examined the different properties of various combinations created by direct metal laser sintering measures<sup>(7-9)</sup>.

Lachmayer et al.<sup>(10)</sup> described the importance of additive manufacturing for manufacture of machine elements. Among varied recognized AM technologies, Selective Laser Melting/Sintering (SLM/SLS) has converted a promising industrial route for engineering parts. Direct Metal Laser Sintering (DMLS) is a fast manufacturing method derived from SLM. It enables prompt modeling of metal substances with defined structure and figure of complex geometry on the basis of virtual 3D model data.

Alsalla and co-authors<sup>(11)</sup> studied the microstructure, surface quality and mechanical behaviour of 316L stainless steel built using selective laser melting process. Microstructural characterization of SLM specimens were carried out by optical and scanning electron microscopy. Mechanical performance of SLM specimens were evaluated by conducting hardness and tensile tests. 316L stainless steel samples were built in YX, XZ and ZX directions. The effect of build direction was minimum on density. Further, build direction played important role in deciding Vickers hardness, tensile and fracture toughness strength. In the investigations all the properties were found more in the samples built in xz directions.

Patrick and Mohsen<sup>(12)</sup> investigated the behaviour of Ti-6Al-4V alloy synthesized by selective laser melting and also studied the influence of build orientations on the various properties. Ti-6Al-4V alloy samples were built in the X, Y and Z directions. The samples developed in X directions exhibited superior tensile properties as compared to Y and Z direction built specimens. The failure mechanisms were studied by the authors and found the brittle mode of fracture features in the area nearer to substrate and ductile fracture features in the area away from the substrate.

Investigations on the mechanical properties of 3D printed carbon fiber reinforced nylon filament were conducted by Flaviana et al.<sup>(13)</sup>. This review investigation the genuine mechanical attributes of parts created with a minimal expense printer from a carbon fiber-supported nylon fiber. The outcomes show that the got values contrast impressively from the qualities introduced in the datasheets of different fiber providers. Also, the hardness and elasticity are impacted by the structure bearing, the infill rate, and the warm burdens, while the flexibility is influenced exclusively by the structure heading. Besides, the connection between the mechanical properties and the filling factor isn't direct.

Kempen et al.<sup>(14)</sup> made comparison between the mechanical properties of AlSi10Mg alloy developed by SLM process and conventional casting process. AlSi10Mg alloy samples were built in two different directions XY and Z orientations using 200W laser power, 1400 mm/s scan speed and 105  $\mu\text{m}$  spacing distance. The samples developed by SLM method exhibited superior tensile strength as compared to conventional cast method. The ultimate tensile strength of conventional cast sample was 300 – 317 MPa, but it was 391-398 MPa in the case of SLM process adopted samples.

In the present research, Al-Mg10-Si alloy developed by SLM process along XY (45°) and Z (90°) orientations. These prepared samples were subjected to microstructural characterization by SEM, EDS and XRD. Mechanical properties like tensile and compression behaviours were evaluated according to ASTM standards.

## 2 Experimental Details

In this study, AlSi10Mg powder was used to prepare the tensile and compression samples using SLM process along XY (45°) and Z (90°) orientations. The powder particle size of the AlSi10Mg was 35 microns. AlSi10Mg powder morphology and chemical composition was carried out using scanning electron microscope and energy dispersive analysis as in Figure 1 and Figure 2 respectively.

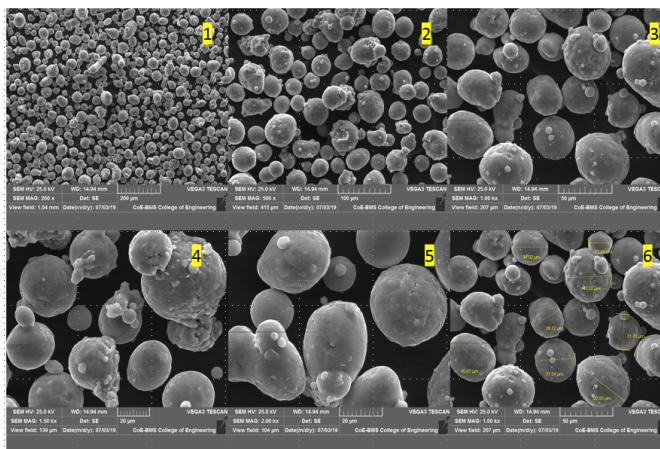


Fig 1. Scanning electron microphotograph of AlSi10Mg powder

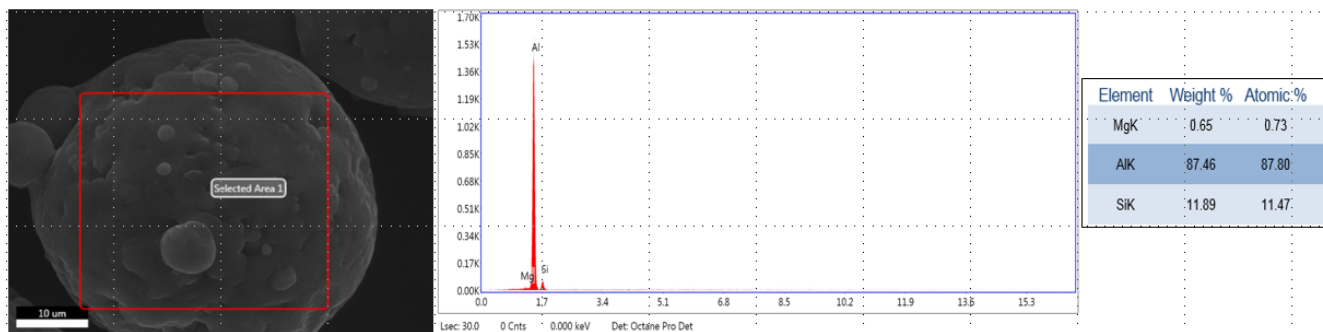


Fig 2. Energy dispersive spectroscopy analysis of AlSi10Mg powder 1 Scanning electron microphotograph of AlSi10Mg powder

Table 1. The chemical composition of AlSi10Mg alloy

Elements	Al	Si	Mg
Weight %	87.46	11.89	0.65

Table 1 is representing the chemical composition of AlSi10Mg powder used to prepare the tensile and compression test specimens. An Al alloy powder particle contains 87.46 wt. % of aluminium, 11.89 wt. % of silicon particles and 0.65 wt. % of magnesium content.

Table 2 is indicating the technical parameters used in the selective laser melting process.

Table 2. Technical parameters of selective laser melting

Parameters	Value
Power	240 W
Scan Speed	1180 mm/s
Layer Thickness	60 μm
Hatch Spacing	0.12 mm
Laser Spot Size	0.1 mm

A series of AlSi10Mg tensile and compression specimens were printed on the stainless steel substrate having built space dimension of 250 mm x 250 mm x 290 mm as shown in the Figure 3. Figure 3 is demonstrating the test specimens on build software. Selective laser melting additive manufacturing machine (EOS M280 Model) with single laser was used to prepare the sample in XY and Z directions. The maximum laser power the EOS M280 machine is 370 W and maximum laser speed is 7000 mmps. In the present investigations tensile and compression specimens were built in XY (45°) and Z (90°) orientations using 240 W laser power, 1180 mm/s scan speed, 60 μm of layer thickness with hatch spacing of 0.12 mm. Prior to printing, the substrates were polished with various grit sized papers and cleaned with ethanol. The layer thickness was 60 μm for every experiment. The fabricating chamber was set at 25 °C initially. The argon gas was supplied into the substrate chamber at 24 L/min of flow rate and 0.05 MPa of pressure to obtain an oxygen level below less than 0.1 %. After achieving a setup oxygen level, the gas supply was cut off and atmosphere in the manufacturing chamber was recycled. Figure 4 (a) shows the as built tensile specimen and Figure 4 (b) indicates the as built compression specimen.

The scanning electron micrographs of arranged AlSi10Mg tests were done utilizing SEM mechanical assembly (TESCAN VEGA, Czech Republic). The device is associated with JED 2300 assessment programming program for EDX examination. For SEM, examples were sliced to get 10 mm in breadth and 5 mm stature. The cut examples were made level surface utilizing belt processor. Then, at that point the examples were cleaned on a progression of silicon carbide emery papers with coarseness size of 300 to 1000. Completing is done by hand on miniature material by fine cerium oxide. Delivered tests were carved to uncover the legitimate granular construction utilizing Keller’s reagent. The carving arrangement comprises of 95 ml of H<sub>2</sub>O, almost 2.5 ml HNO<sub>3</sub>, likewise 1.5 ml HCl and 1 ml HF.

By the use of automated universal testing machine (UTM) of Instron make, with 60 kN ability with least count of 4 N, malleable tests were done. The ductile examples having a component of 30 mm check length were utilized according to ASTM E8<sup>(15)</sup> standard. After the test, crack surfaces are introduced for microstructural concentrates on utilizing SEM to comprehend the break system. Compression tests were carried out on 20 mm diameter and 60 mm length as built specimens as per ASTM

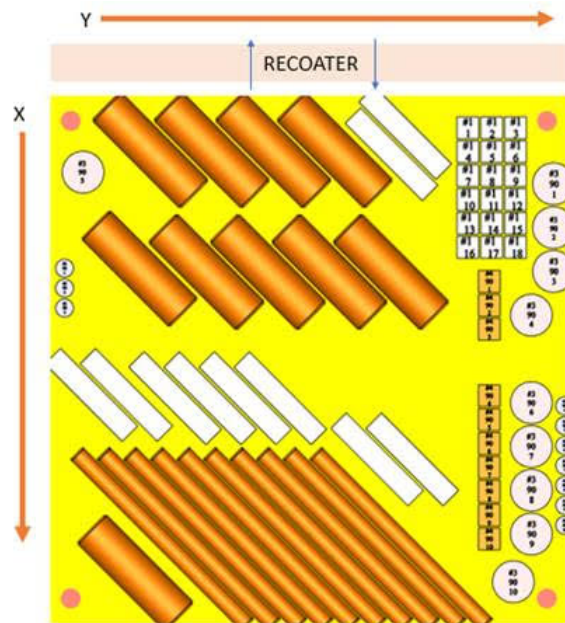


Fig 3. Test specimens on build software



(a)



(b)

Fig 4. Showing (a) as built tensile specimen (b) as built compression specimen

E9<sup>(16)</sup> standard. On each orientations three samples were tested for tensile and compression, average reading was tabulated in the graphs using error bars.

### 3 Results and Discussion

#### 3.1 Microstructural Analysis

Figure 5 shows microstructures of XY (45°) and Z (90°) built samples in the perpendicular to the build direction i.e., for XY (45°) prepared samples SEM analysis were carried out on XZ surface as in Figure 5 (a) and for Z (90°) built sample it was along Z direction. Densification is little more complete in the XY direction, since Figure 5 (a) exhibits voids and pores free surface; this is mainly due to proper melting of AlSi10Mg particles along the XY direction. Further, small pores found in Z direction built samples which can be explained through three different sources i) incomplete melting ii) shrinkage and iii) the composition of gas voids. In Figure 5 it was observed that the pores in the Z direction built samples have an irregular shape and appear more frequently than in XY direction built samples. The properties of samples mainly depending on the microstructures obtained, if

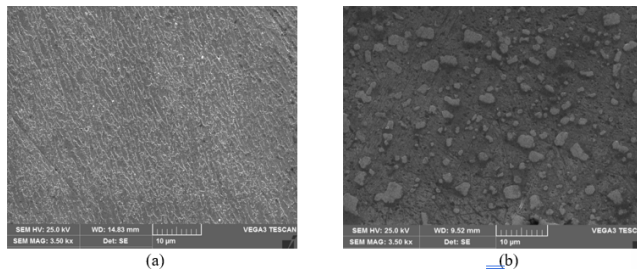


Fig 5. Scanning electron microphotographs of (a) XZ direction (b) Z direction

SEM micrographs are free from voids, which showing the complete melting of particles and enhances the strength.

### 3.2 Tensile Properties

Table 3. Tensile properties

Built Orientation	Ultimate Tensile Strength (MPa)	Yield Strength (MPa)	Elongation (%)
XY (45°)	439.79	363.7	6.72
	422.72	384.4	6.08
	423.39	376.4	6.36
Z (90°)	444.60	370.4	6.60
	378.40	347.8	5.32
	401.91	355.8	5.16

Figure 6 and Table 3 reveal the ultimate tensile strength that was obtained for the XY and Z directions built samples. From the Table 3, the highest ultimate strength was recorded for the samples built in XY (45°) orientation. The ultimate strength of samples prepared in the XY directions are 439.79 MPa, 422.7 MPa and 423.3 MPa. The differences were obtained between each reading is very minimal and average ultimate tensile strength obtained in XY direction built sample is 428.6 MPa. Further, Z (90°) built samples exhibited lesser ultimate tensile strength as compared to the XY direction built samples. The average ultimate strength found in Z direction built sample is 408.3 MPa. These results are similar to Alsalla and co-authors<sup>(11)</sup> that carried out the experiments on 316L stainless steel developed by selective laser melting process.

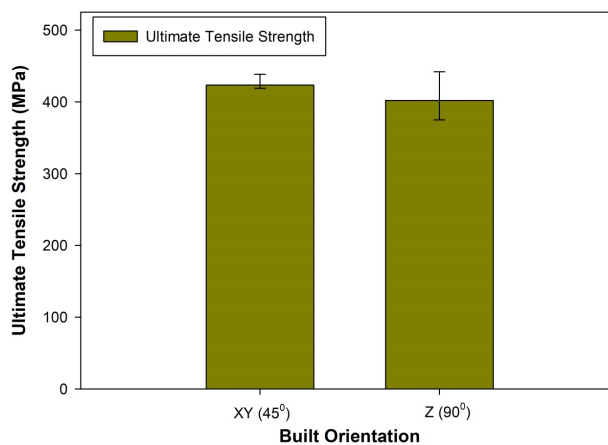


Fig 6. Ultimate strength of XY and Z orientations built AlSi10Mg samples

Figure 7 and Figure 7 are demonstrating the ultimate and yield strength of AlSi10Mg samples prepared by selective laser melting process in XY and Z built orientations. From these figures it is noted that the samples built in the XY direction show the highest ultimate and yield strength. However, there is slight difference in the yield strength of both samples built in XY and Z directions. This highest ultimate strength in the XY built direction sample is owing to fewer pores and voids being present and finer grains as in Figure 5 (a). The lesser ultimate strength in Z direction built samples is due to presence of defects, such as cracks and pores; these can be eliminated or reduced by performing secondary operations.

The differences in the ultimate, yield and percentage elongation (Figure 8) values obtained in this study with different build directions had been anticipated by the previous investigations based on the microstructural analysis. The tensile test results also showed that the samples built in the XY direction recorded highest values of UTS and elongation (Figure 8), meaning that there is a larger area under the stress strain curve, which indicates the material absorbs more energy before failure. These results indicate that the built orientation has strong effect upon the properties.

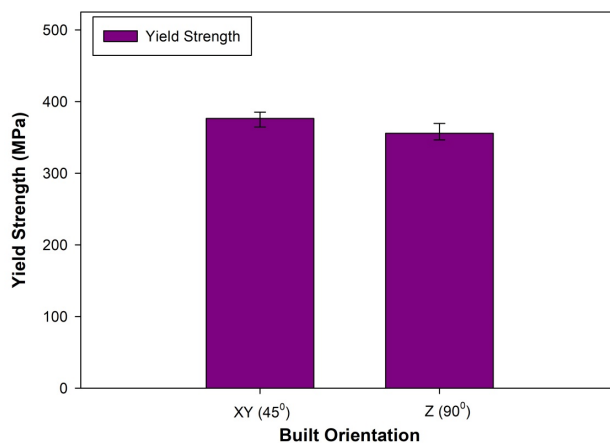


Fig 7. Yield strength of XY and Z orientations built AlSi10Mg samples

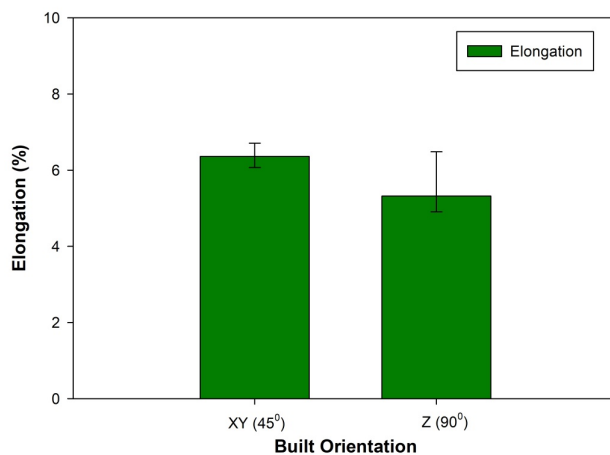


Fig 8. Elongation (%) of XY and Z orientations built AlSi10Mg samples

### 3.3 Compression Strength

Table 4 Compression strength of samples prepared using selective laser melting process

**Table 4. Compression strength of samples prepared using selective laser melting process**

Built Orientation	Compression Strength (MPa)
XY (45°)	641.14
	640.32
	646.58
Z (90°)	636.74
	638.40
	641.17

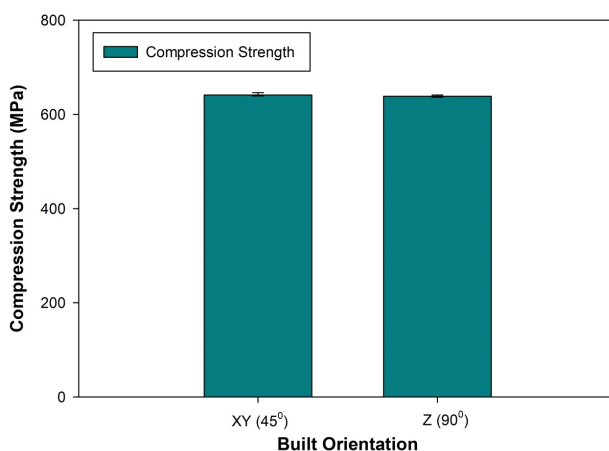


**Fig 9. Compression strength of XY and Z orientations built AlSi10Mg samples**

Table 4 and Figure 8 are representing the compression strength of AlSi10Mg samples prepared by selective laser melting process in XY (45°) and Z (90°) orientations. The compression strength of XY direction built samples is 641.14 MPa, 640.32 MPa and 646.58 MPa with average compression strength value of 642.68 MPa. Further, the compression strength of Z direction built samples is showing 636.74 MPa, 638.40 MPa and 641.17 MPa with average compression strength of 638.77 MPa. The enhanced compression strength is observed in the case of XY (45°) direction built samples as compared to Z (90°) orientation built samples. This is mainly due to proper densification is observed in the case of XY direction built samples. Byron and co-authors<sup>(17)</sup> justified the importance of build orientation on the properties of metal materials prepared by additive manufacturing process.

## 4 Conclusions

In the present research AlSi10Mg samples for microstructure, tensile and compression strengths evaluation were developed using selective laser melting process in XY (45°) and Z (90°) build orientations. The prepared samples were evaluated for tensile and compression properties as per ASTM E8 and E9 standards respectively. Very few investigators investigated the properties of AlSi10Mg alloy developed in XY (45°) orientations. In the current study also samples developed in XY (45°) orientations exhibited superior tensile properties like ultimate, yield and percentage elongation along with enhancement in compression strength. Hence, AlSi10Mg alloy components for automotive industries can be developed by using SLM process in XY (45°) build orientation.

## References

- 1) Gokuldoss SPK, Kolla J, Eckert. Additive manufacturing processes: Selective laser melting, electron beam melting and binder jetting-selection guidelines. *Materials*. 2017;10(672). doi:10.3390/ma10060672.
- 2) Matti S, Siddesh, Shivakumar BP, Shashidhar S. Dry sliding wear behavior of mica, fly ash and red mud particles reinforced Al7075 alloy hybrid metal matrix composites. *Indian Journal of Science and Technology*. 2021;14(4):310–318. doi:10.17485/IJST/v14i4.2081.
- 3) Gokuldoss PK. Selective laser melting: Materials and applications. *Journal of Manufacturing and Materials Processing*. 2020;4(13). doi:10.3390/jmmp4010013.
- 4) Sert E, Hitzler L, Hafenstein S. Tensile and compressive behaviour of additively manufactured AlSi10Mg samples. *Prog Addit Manuf*. 2020;5:305–313. doi:10.1007/s40964-020-00131-9.
- 5) Ponnusamy P, Rashid RAR, Masood SH, Ruan D, Palanisamy S. Mechanical Properties of SLM-Printed Aluminium Alloys. *A Review Materials*. 2020;13:4301–4301. doi:10.3390/ma13194301.
- 6) Li YFZH, Nie B, Liu ZZ, Kuai M, Zhao F, Liu. Mechanical properties of AlSi10Mg lattice structures fabricated by selective laser melting. *Materials & Design*. 2020;19. doi:10.1016/j.matdes.2020.108709.
- 7) Yan Q, Song B, Shi Y. Comparative study of performance comparison of AlSi10Mg alloy prepared by selective laser melting and casting. *Journal of Materials Science & Technology*. 2020;41(0):199–208. doi:10.1016/j.jmst.2019.08.049.
- 8) Gu XH, Zhang JX, Fan XL, Zhang LC. Corrosion Behavior of Selective Laser Melted AlSi10Mg Alloy in NaCl Solution and Its Dependence on Heat Treatment. *Acta Metallurgica Sinica (English Letters)*. 2019;33(3):327–337. doi:10.1007/s40195-019-00903-5.
- 9) Murphy D, Michael. Performance evaluation of AlSi10Mg fabricated by a selective laser melting process. 2020. Available from: [https://scholarsmine.mst.edu/masters\\_theses/8006](https://scholarsmine.mst.edu/masters_theses/8006).
- 10) Lachmayer R, Zghair C, Klose F, Nurnberger. Introducing selective laser melting to manufacture machine elements. *International Design Conference*. 2016;p. 831–842.
- 11) Alsalla HH, Smith C, Hao L. Effect of build orientation on the surface quality, microstructure and mechanical properties of selective laser melting 316L stainless steel. *Rapid Prototyping Journal*. 2018;24(1):9–17. doi:10.1108/rpj-04-2016-0068.
- 12) Hartunian P, Eshraghi M. Effect of Build Orientation on the Microstructure and Mechanical Properties of Selective Laser-Melted Ti-6Al-4V Alloy. *Journal of Manufacturing and Materials Processing*. 2018;2(4):69–69. doi:10.3390/jmmp2040069.
- 13) Calignano F, Lorusso M, Roppolo I, Minetola P. Investigation of the Mechanical Properties of a Carbon Fibre-Reinforced Nylon Filament for 3D Printing. *Machines*. 2020;8(3):52–52. Available from: <https://dx.doi.org/10.3390/machines8030052>. doi:10.3390/machines8030052.
- 14) Kempen K, Thijs L, Humbeek JPV, Kruth JP. Mechanical Properties of AlSi10Mg Produced by Selective Laser Melting. *Physics Procedia*. 2012;39:439–446. doi:10.1016/j.phpro.2012.10.059.
- 15) Dama K, Prashanth L, Nagaral M, Mathapati R, Hanumantharayagouda MB. Microstructure and Mechanical Behavior of B4C Particulates Reinforced ZA27 Alloy Composites. *Materials Today: Proceedings*. 2017;4(8):7546–7553. doi:10.1016/j.matpr.2017.07.086.
- 16) Jadhav BRPR, Sridhar M, Nagaral, Harti. Evaluation of mechanical properties of B4C and graphite particulates reinforced A356 alloy hybrid composites. *Materials Today: Proceedings*. 2017;4(9):9972–9976. doi:10.1016/j.matpr.2017.06.304.
- 17) Milner BB, Gradl P, Snedden G, Brooks M, Pitot J, Lopez E, et al. Anton du Plessis. Metal additive manufacturing in aerospace: A review. *Materials & Design*. 2021;110008:209–209. doi:10.1016/j.matdes.2021.110008.